ELSEVIER

Journal of Photochemistry and Photobiology A: Chemistry 117 (1998) 175–184

Journal of Photochemistry and Photobiology A:Chemistry

# Time-resolved fluorescence spectroscopy of fulvic acid and fulvic acid complexed with $Eu^{3+}$ – a comparative study

C.-D. Tiseanu[1,a], M.U. Kumke[a], F.H. Frimmel[a,*], R. Klenze[b], J.I. Kim[b]

[a] *Engler-Bunte Institute, Division of Water Chemistry, Univerity of Karlsruhe, Richard-Willstätter-Allee 5, 76131 Karlsruhe, Germany*

[b] *Forschungszentrum Karlsruhe, Institut für Nukleare Entsorgungstechnik, 76126 Karlsruhe, Germany*

Received 30 March 1998; received in revised form 22 June 1998; accepted 24 June 1998

**Abstract**

In this work a systematic characterization of the fluorescence kinetics of fulvic acid by means of a single-photon time correlation technique is reported. The data were extracted from both single decay curves and time-resolved emission spectra and analyzed by the exponential series method. The results strongly suggest the existence of a tri-modal decay time distribution with peak decay time values centred around 0.7, 3 and 10 ns. The relative amplitudes of the decay time distributions were shown to depend on the emission wavelength, indicating a three-species mixture with slightly different emission maxima and widths. As sustained by time-resolved emission spectra the same species of fluorophores are responsible for the fluorescence kinetics behaviour of fulvic acid at all excitation wavelengths used in the experiments. For the first time these techniques and methods were applied in investigating the effects of the $Eu^{3+}$ complexation upon fluorescence kinetics of the fulvic acid. Single decay analysis indicates that the peak decay time values are not affected by $Eu^{3+}$ addition at all emission and excitation wavelengths used in the experiments. On the contrary, the dependency of relative amplitudes on emission wavelength was greatly reduced in comparison with the uncomplexed fulvic acid. This effect is further evidenced by analysing the barycenter transients of time-resolved emission spectra. Finally, it is also indicated that within the temporal resolution of the experimental set up used the singlet states play no role as donor states in intramolecular energy transfer from the organic fulvic acid ligands to the $Eu^{3+}$ energy levels. 

*Keywords:* Time-resolved fluorescence; Fulvic acid; Europium ion

## 1. Introduction

Humic substances (HS) – humic acids (HA) and fulvic acids (FA) – are macromolecular compounds with a very complex and heterogeneous structure that show polyfunctional, polyelectrolytic and conformationally related properties [1–4]. Consequently, the fluorescence of dissolved HS depends strongly on their origin, molecular weight, concentration, pH, ionic strength, temperature, redox potential of the medium and finally on the interactions with organic xenobiotics and anorganic constituents, e.g. metal ions [5,6].

During the last decade fluorescence spectroscopy has been successfully applied in extracting useful information on quantitative and qualitative aspects of HS. However, only little reliable data on the dynamic fluorescence behaviour of HS (e.g. fluorescence decay times, time-resolved fluorescence emission spectra (TRES)) have been reported in the literature.

Recently, the maximum entropy method (MEM) was used for the data analysis of FA fluorescence decays indicating a tri-modal fluorescence decay times distribution for the investigated FA [7]. The peak decay time values reported were around 1, 3 and 10 ns. In a more detailed study [8], HS from different aquatic origins were investigated by means of a different deconvolution algorithm (exponential series method, ESM), and again a tri-modal distribution with similar peak decay time values was found for the investigated HS as well. The study proved the applicability of time-resolved fluorescence measurements for the investigation of the molecular dynamics of humic substances. A suggestion to relate certain parts of the calculated fluorescence decay time distribution with structural subunits of the investigated humic substances was made.

The acidic functional groups of HS are an abundant source of metal binding sites in the natural environment. Studies of metal binding to HS are of great environmental interest because of the biological and physicochemical

*Corresponding author. E-mail: fritz.frimmel@ciw.uni-karlsruhe.de

[1]Present address: Institute of Atomic Physics, Solid State Quantum Electronics Laboratory, POB MG-36, R-76900 Bucharest, Romania.

1010-6030/98/$ – see front matter 
PII: S1010-6030(98)00336-0

properties of metals which are often dramatically changed as a result of complexation by HS [9,10].

In order to understand how these heterogeneous organic macromolecules bind metals within a large range of binding energies, TRES has been used to study changes in the luminescence spectra of lanthanide metal ion when binding to HS. The study of sensitised fluorescence by energy transfer from the excited chromophores to the *f*-element ion may yield, among others, information about binding distance between the organic ligand and the metal ion. One of the metals most extensively studied is the $Eu^{3+}$ ion. As reported by other authors, Eu binding to humic substances resulted in sensitised $Eu^{3+}$ luminescence following the intramolecular energy transfer (IMET) from HS ligands to Eu excited levels [11–16]. The 'traditional' picture of IMET is based on the donor character of the triplet state of the organic ligands which transfers the excitation energy through a dipole–dipole interaction mechanism to the excited $Eu^{3+}$ levels. For a recent review on IMET, see, for example, reference [17].

This assumption, however, lacks two important experimental evidences: (a) the impossibility of observing the phosphorescence of the donor (e.g. the triplet state of HS) at room temperature and in solution due to strong quenching processes. In other words, no experimental observations of the dynamic effect of energy transfer manifested as a fast initial drop in the luminescence kinetics of the HS donor could be extracted; (b) no effects of the energy transfer may be inferred from the acceptor ($Eu^{3+}$) luminescence as well, within the usual temporal resolution reported in such studies.

Our preliminary results obtained in a different series of TRES experiments (details will be published elsewhere) indicate that the rate of the energy transfer from FA to $Eu^{3+}$ is faster than the temporal resolution of the instrumental set up (approx. 10 ns) e.g., larger than $10^{-7}$–$10^{-8}$ $s^{-1}$. In this case, quantitative estimations of the energy transfer from the acceptor ($Eu^{3+}$) luminescence kinetics were not possible, as no rise time in $Eu^{3+}$-sensitised luminescence was detected.

Moreover, the mechanism of IMET from the donor triplet state to most of the excited state levels of the lanthanide ions is a (super)exchange one as imposed by the Wigner–Pauli rule [17,18]. In this case, information on distances between ligand and metal ion commonly obtained within the Foerster–Dexter formalism is not straightforward to obtain [19]. However, this rule may be relaxed in case of the mixing of the triplet states with energetically closely situated singlet states.

To the difficulties one usually encounters in TRES studies concerning interactions between HS and $Eu^{3+}$ ions (as well as other lanthanides and actinide ions), we must add the lack of reliable data concerning the effects induced by lanthanide ions on the fluorescence kinetics of humic substances.

There are three issues we investigate in this paper: (1) the kinetics of the FA fluorescence and its dependence on excitation wavelength, emission wavelength and FA concentration, (2) the effects induced by $Eu^{3+}$ binding on the FA fluorescence kinetics, and (3) the possible role of FA singlet states as a donor state for an energy transfer from FA ligands to $Eu^{3+}$. The latter issue was imposed by (a) the dense scheme of excited energy levels presented by $Eu^{3+}$ in the region of FA fluorescence (e.g. between 390 and 550 nm) [20] and (b) some earlier observations according to which in some of the lanthanide complexes, the IMET process seems to occur through a direct resonance energy transfer between a ligand singlet level and a lanthanide ion level [21]

## 2. Experimental details

The time-resolved fluorescence measurements were performed using a FL900CDT fluorescence decay time spectrometer (Edinburgh Analytical Instruments, UK) in the time-correlated single photon counting mode. The instrument was set up in a T-geometry format with two analyzing detection channels. The grating of the excitation monochromator was blazed at 250 nm and the grating of the emission monochromators was blazed at 500 nm for optimal performance. The linear dispersion of the monochromators was 1.8 nm/mm which determined together with the slit width the spectral bandpass of the fluorescence measurements. For the detection photomultiplier tubes (PMT) R1527 (Hamamatsu) with a typical rise time of 2.2 ns were used. A nF900 ns flash lamp (Edinburgh Analytical Instruments) filled with nitrogen gas was used for the excitation of the samples. The multichannel analyser (MCA) Norland 5000 (Viking Instruments, USA) was operated in the pulse height analysis mode. The memory of the MCA Norland 5000 consists of 4096 channels. In the typical T-geometry format experiment 1024 channels of the MCA were attributed to each detection channel.

For data analysis the commercial software package of Edinburgh Instruments was applied based on the ESM approach and on the discrete components approach (DCA). For a reliable data evaluation of complex fluorescence kinetics the acquisition rate (reported as the count rate at peak maximum) is a crucial parameter. Experiments at different levels of counts ($10^3$–$10^5$ counts at the peak maximum) were performed and the influence on fitting results was monitored.

The measurement time was usually below 4 h, and the stability of the time profile of the excitation pulse was controlled by monitoring the fluorescence decay of the NOM samples and the excitation pulse in cycles of 5000 counts per cycle. In general, the counting rate was less than 1% for the natural organic matter samples under investigation and therefore pile-up problems in decay time analysis were not likely to occur.

The excitation wavelengths in the time-resolved fluorescence experiments were 314, 357 and 379 nm. The experiments were typically run at a time base of 100 ns with

5 ns delay of the stop PMT. Fluorescence emission was detected between 380 and 580 nm with a spectral bandwidth of 9 nm.

Steady-state fluorescence measurements were performed with a Perkin–Elmer LS 5B spectrofluorometer. In the standard steady-state experiments a spectral bandwidth of 10 nm in excitation and emission was used. Excitation wavelengths of 314 nm were applied and the spectra were recorded in the range between 350 and 600 nm. The spectra were background corrected and for comparison purposes normalized to the dissolved organic carbon concentration (DOC, in mg/l). The Raman signal of pure water was used as internal standard for the correction of day-to-day fluctuations of excitation intensity. The fluorescence intensities were not corrected for the inner filter effects nor for the spectral difference of the PMT response because the spectra were evaluated on a relative base and no change in the shape of fulvic acid fluorescence was observed under experimental conditions.

The fulvic acid fraction under investigation was extracted from one of the deep ground waters in Gorleben area in northern Germany. Details of the extraction and purification as well as basic data can be found elsewhere [22]. Stock solutions of $Eu^{3+}$ were prepared by dissolving $Eu_2O_3$ in 0.1 M $HClO_4$ and dilution with 0.1 M $NaClO_4$. The pH for pure and complexed FA samples was adjusted to approx. 6, and the concentration of $Eu^{3+}$ was kept in all time-resolved fluorescence experiments at $10^{-4}$ M.

Fluorescence was monitored for a DOC in the range between 5 and 30 mg/l in steps of 5 mg/l. In general, the influence of $Eu^{3+}$ on FA fluorescence decay was monitored for a DOC of 10 mg/l. All fluorescence measurements were performed at room temperature.

## 3. Results

The time dependence of the fluorescence intensity $I(t)$ was measured and the data were analyzed using three discrete exponential terms (DCA) and with a distributional analysis based on the ESM, [23,24].

$$I(t) = \int_0^\infty A(\tau)\exp(-t/\tau)\mathrm{d}\tau \quad (1)$$

In this approach up to 100 decay times ranging from 0.1 to 50 ns equally spaced in the logarithmic time scale were used. The amplitude distribution $A(\tau)$ recovered by the ESM represents the maximum probability of amplitudes among the decay time components. The quality of the exponential fit was determined from the randomness of the weighted residuals distribution at $\chi^2$ close to unity. The parameters of fluorescence decay obtained by the ESM are defined as follows: (a) the distribution $A(\tau)$ is divided in as many peaks (or decay components) as can be clearly separated by two successive well-defined minima; (b) the peak decay time values, $\tau_i$, represent the average position of the peak $i$ in ns, calculated as:

$$\tau_i = \sum_j A_j\tau_j / \sum_j A_j \quad (2)$$

calculated over all decay times $j$ included in the peak $i$; the relative amplitude $A_i$ is the ratio of the peak surface $\sum A_j$ over the entire surface of the distribution. The ESM analysis also provides the distribution width parameters reflecting both the degree of inhomogeneity experienced by fluorescing species and noise effects. The experimental data consist of a convolved decay curve, and thus the ESM recovery curve, $I(t)$, is obtained by iterative re-convolution with the instrumental response function.

To obtain accurate fluorescence decay parameters, the following steps were used: the visual inspection of the experimental decay curves to establish the best fitting range; DCA fit and ESM analysis together with choosing between the optimum of the $\chi^2$ values and the best images of the residuals.

### 3.1. Single decay curves analysis

#### 3.1.1. Dependence of the fluorescence decay of FA and FA complexed with $Eu^{3+}$ on the excitation wavelength

*FA*: The FA fluorescence was excited at three excitation wavelengths $\lambda_{ex}$=314, 357 and 379 nm, the first two wavelengths were chosen around the maximum of the fluorescence excitation spectrum of the FA and the third wavelength was selected at the red edge of the fluorescence excitation spectrum (see Fig. 1).

Within the experimental spectral resolution, the shape of FA excitation spectra were minimally changed upon complexation with $Eu^{3+}$: there were only second-order

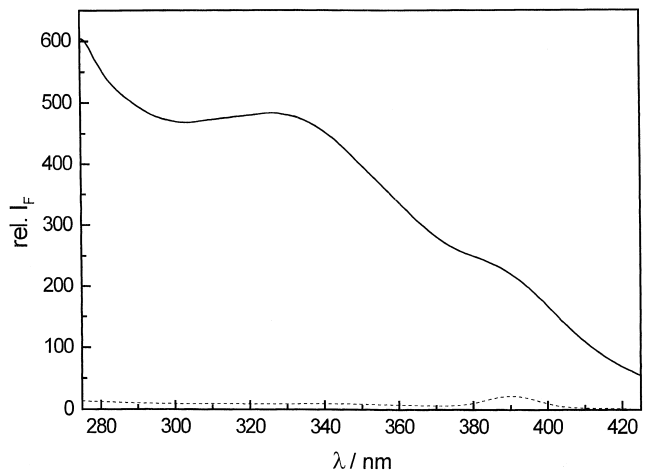


Fig. 1. Excitation spectrum of the FA at room temperature (emission wavelength is 450 nm). The excitation and the emission slit widths were 10 nm. The dotted line represents the background fluorescence spectrum of water.

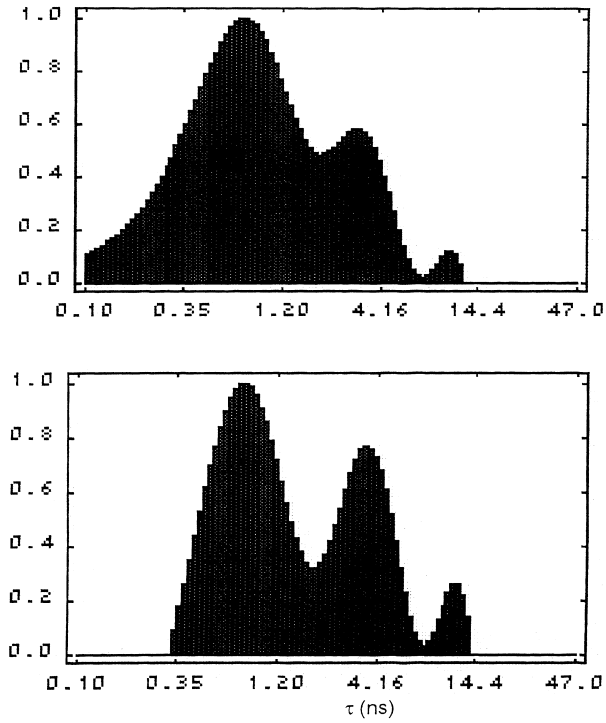


Fig. 2. The fluorescence lifetimes distribution of the FA recovered by ESM. Excitation wavelength: 314 nm (bandwidth 10 nm). Temperature 18°C. Above: $\lambda_{em}$=390 nm; $4\times10^4$ counts in the peak channel. The corresponding $\chi^2$ value was 1.037. Below: $\lambda_{em}$=530 nm; $4\times10^4$ counts in the peak channel. The corresponding $\chi^2$ value was 1.098. Fluorescence decay parameters values are listed in Table 1.

changes observed in the difference spectrum (figure not shown). These changes may involve increased intensities of certain modes but no changes in the eigenvalues of the FA states.

In most cases, the decay time distributions obtained with the ESM analysis had a three modes pattern with the corresponding peak decay times centred around the following values: 0.7–1; 3–3.6 and 8–10 ns with $\lambda_{ex}$=314 nm (Fig. 2) and three to four peak decay times centred around 0.7–0.9, 2.2–2.7, 5–6 ns and 15 ns with $\lambda_{ex}$=357 nm, respectively. At an excitation wavelength of 357 nm a fourth decay time component appeared that could not be neglected, as its relative amplitude was around 10% for emission wavelengths larger than 450 nm. At an excitation wavelength of 379 nm the decay parameters for the emission wavelengths $\lambda_{em}$=390 nm and $\lambda_{em}$=420 nm were comparable with those obtained with $\lambda_{ex}$=314 nm.

Table 1 summarises the fluorescence decay parameters found for the FA under different excitation wavelengths. The results for peak decay time values, the relative amplitudes and the mean decay times recovered by the ESM analysis are also shown. Within certain limits, these results witness the absence of a significant excitation wavelength dependence of the fluorescence decay time distribution. The ESM results are in satisfactory agreement with the results recovered by DCA (three-exponential fitting).

*FA complexed with $Eu^{3+}$*: In the time-resolved fluorescence experiments the concentration was $10^{-4}$ M. At this $Eu^{3+}$ concentration all metal binding sites were saturated.

Similar with the case of FA, the ESM results concerning the fluorescence kinetics of FA complexed with $Eu^{3+}$ did not reveal significant changes with the excitation wavelength. At each excitation wavelength a three-modes decay times distribution was calculated, the peak decay-times values being unchanged in comparison with the values obtained without $Eu^{3+}$. For illustration, in Table 2 the decay parameters obtained at $\lambda_{ex}$=314 nm are listed. The ESM results are also in satisfactory agreement with the results recovered by DCA (three-exponential fitting).

### 3.1.2. Dependence of the fluorescence decay of FA and FA complexed with $Eu^{3+}$ on the emission wavelength

*FA*: All the measured fluorescence decays were highly non-exponential and showed a large variation as the emission wavelength $\lambda_{em}$ was varied in the range between 390 and 550 nm. The mean decay times at $\lambda_{ex}$=314 and 357 nm increased up to 50% and 200%, respectively (see Table 1). At $\lambda_{ex}$=379 nm the fluorescence decay was measured at two emission wavelengths 390 and 420 nm. Therefore no trend of the mean decay time over the emission range could be inferred. Below, we resume the results obtained with $\lambda_{ex}$=314 nm, with the emphasis that these results could also be regarded representative for $\lambda_{ex}$=357 nm, and for $\lambda_{ex}$=379 nm: (a) all peak decay time values showed a slight shift in the same direction (towards larger values) with increasing emission wavelengths. However, due to experimental and method calculation errors this trend has to be judged very carefully. (b) there was a continuous redistribution of the relative amplitudes between the shortest and the longest decay time values, in a sense that the latter is favoured at longer emission wavelengths. The second decay constant represented the majority of the fluorescence decay components and it showed only a slight variation of its relative amplitude (about 45–55%) over the measured emission wavelength range. Therefore, variation of the FA fluorescence mean decay time across the emission spectrum could be related to changes in the relative amplitudes of the first and the third component of fluorescence decay. At $\lambda_{ex}$=357 nm and for emission wavelengths larger than 450 nm, the middle decay time components, centred around 2 and 6 ns, redistributed their relative amplitudes in the sense that the 6 ns decay time became favoured at longer emission wavelengths. (c) There was a significant contribution to the decay time distribution at short decay times (up to 35–40%) at the blue edge of the emission spectrum at $\lambda_{ex}$=314 nm and up to 30% at $\lambda_{ex}$=357 nm. This feature is typical of FA from different origins [8] and, as resulted from our data, this parameter did not vary with the concentration of the FA. (d) For the longest decay component obtained at $\lambda_{ex}$=314 nm there was a larger dispersion of its values between 6 and 10 ns, most probably due to the noise effects which imposed different final fitting range values in

Table 1
Dependence of the fluorescence decay parameters of FA on the emission wavelength recovered by ESM (excitation wavelengths $\lambda_{ex}$=314, 357 and 379 nm, temperature 18°C)

| $\lambda_{ex}$ (nm) | $\lambda_{em}$ (nm) | Peak decay times, $\tau_i$ (ns) and relative $A_i$ (%) | | | | $\tau_{mean}$[a] (ns) | $\chi^2$ |
|---|---|---|---|---|---|---|---|
| 314 | 390 | 0.7±0.3 | 3.1±0.9 | 9±1.1 | | 5.2 | 1.037 |
| | | 36 | 51 | 13 | | | |
| 357 | 390 | 0.7±0.4 | 2.2±1 | 6.1±1.2 | | 4.1 | 1.065 |
| | | 31 | 46 | 21 | | | |
| 314 | 420 | 0.8±0.5 | 3.3±1.1 | 10±1.5 | | 6.2 | 1.074 |
| | | 27 | 56 | 17 | | | |
| 357 | 420 | 0.7±0.3 | 2.3±0.9 | 6±0.6 | 16±1.2 | 6.9 | 0.985 |
| | | 21 | 46 | 28 | 5 | | |
| 379 | 420 | 1±0.6 | 3.2±1.1 | 8.5±1.4 | | 5 | 1.121 |
| | | 39 | 47 | 14.5 | | | |
| 314 | 450 | 0.8±0.5 | 3±0.9 | 8±0.9 | | 5.7 | 1.034 |
| | | 25 | 49 | 26 | | | |
| 357 | 450 | 0.9±0.6 | 2.5±1.2 | 5.5±1 | 15±2.5 | 7.3 | 1.155 |
| | | 23 | 35 | 34 | 8 | | |
| 379 | 450 | 1±0.5 | 3.2±0.6 | 8±0.8 | | 5.4 | 1.023 |
| | | 27 | 48 | 22 | | | |
| 314 | 490 | 0.9±0.6 | 3.3±1.2 | 9±1.5 | | 6.4 | 1.046 |
| | | 22 | 51 | 27 | | | |
| 357 | 490 | 0.7±0.4 | 2.2±0.8 | 5.1±0.9 | 15 | 8.5 | 1.080 |
| | | 13 | 34 | 39 | 10 | | |
| 314 | 530 | 1±0.6 | 3.2±0.9 | 9±1.1 | | 6.7 | 1.098 |
| | | 18 | 52 | 30 | | | |
| 357 | 530 | 0.8±0.6 | 2.7±0.8 | 6.5±0.9 | 15±2.4 | 8.5 | 1.043 |
| | | 13 | 40 | 35 | 12 | | |
| 314 | 550 | 1±0.5 | 3.6±0.6 | 10±1.2 | | 7.5 | 1.025 |
| | | 16 | 51 | 33 | | | |
| 357 | 550 | 0.8±0.7 | 2.2±1.2 | 5.7±1.4 | 16±2.6 | 8.8 | 1.117 |
| | | 14 | 32 | 43 | 10 | | |

[a] $\tau_{mean}$ is calculated according to equation: $\tau_{mean} = \sum A_i\tau_i^2 / \sum A_i\tau_i$, which emphasises the long time component of the decay function.

each of the cases. (e) All values of relative amplitudes were positive over the whole emission range studied, i.e. no tendency to negative values for the third amplitude was observed, even for emission wavelengths longer than 500 nm. (f) The decay parameters were invariant with FA concentration in the range between 5 and 15 mg/l dissolved organic carbon (DOC).

*FA complexed with $Eu^{3+}$*: In contrast to the slight dependency of the decay parameters of FA complexed with $Eu^{3+}$ on the excitation wavelength, the variation of the emission wavelength gave strong differences relative to the FA fluorescence mainly at the blue and the red edges of the emission spectra. To illustrate these changes, in Fig. 3 the decay curves of FA and FA complexed with $Eu^{3+}$ are presented, measured at the spectral edges of the emission spectra at $\lambda_{ex}$=314 nm

Table 2
Fluorescence decay parameters of FA complexed with $Eu^{3+}$ at different emission wavelengths (excitation wavelength $\lambda_{ex}$=314 nm, temperature 18°C, ($(Eu^{3+})=10^{-4}$ M)

| $\lambda_{em}$(nm) | Peak decay times, $\tau_i$ (ns) and relative $A_i$ (%) | | | $\tau_{mean}$ (ns) | $\chi^2$ |
|---|---|---|---|---|---|
| 390 | 0.7±0.5 | 3.2±0.7 | 11±0.8 | 6.9 | 1.037 |
| | 29 | 54 | 17 | | |
| 420 | 0.7±0.6 | 3.1±0.9 | 11±1.1 | 7.2 | 1.074 |
| | 26 | 55 | 19 | | |
| 450 | 0.75±0.5 | 3.2±0.8 | 10±1.1 | 7.7 | 1.034 |
| | 26 | 50 | 24 | | |
| 530 | 0.8±0.5 | 3.2±1.1 | 11±1.4 | 7.7 | 1.098 |
| | 27 | 49 | 24 | | |

$\tau_{mean}$ is calculated as shown in Table 1.

As shown in Fig. 3, the effects of $Eu^{3+}$ complexation on FA fluorescence kinetics can be resumed as follows: (1) at the blue edge (390 nm), the kinetics of FA in the presence of $Eu^{3+}$ was slowed down in the first approx. 20 ns while for times longer than approx. 40 ns the kinetics was accelerated; (2) at the red edge of the emission spectra (530 nm), the opposite effect was observed and (3) the effect of $Eu^{3+}$ on FA fluorescence kinetics was stronger with decreasing emission wavelengths (Tables 1 and 2, Fig. 3).

Upon the addition of $Eu^{3+}$, we found that the differences in FA fluorescence decay times between the extremes of the emission range investigated were strongly reduced; a surprising result if one takes into account the strong variation of FA fluorescence kinetics with emission wavelength. For comparison, in Fig. 4 the experimental decay curves of FA and FA complexed with $Eu^{3+}$ are shown measured at $\lambda_{em}$=390 nm and 530 nm with $\lambda_{ex}$=314 nm.

As expected, the decay parameters for FA complexed with $Eu^{3+}$ showed a only slight dependence on the emission

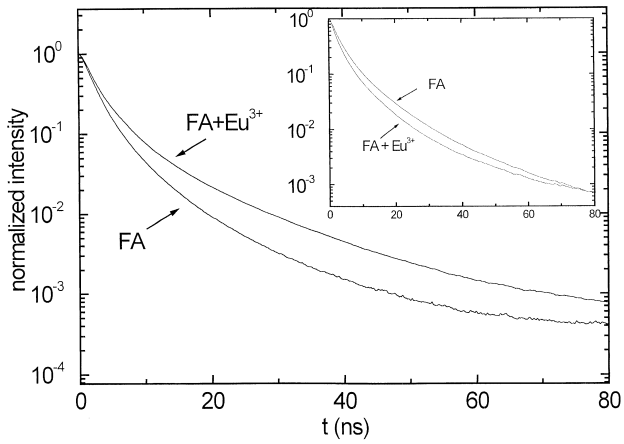


Fig. 3. The fluorescence kinetics of the FA and FA complexed with $Eu^{3+}$ excited at 314 nm and measured at 390 nm. The insert shows the fluorescence kinetics of the FA and FA complexed with $Eu^{3}$ measured at 530 nm. ($(Eu^{3+})=10^{-4}$ M). All curves represent the fits of the experimental fluorescence decays to a three-exponential function.

wavelength for the decay time distribution with the peak decay time values centred at 0.7, 3.1 and 11 ns, and the relative amplitudes of 27–29%, 49–54% and 17–24%, respectively (Table 2). Also, the mean decay times varied only slightly with emission wavelength: 10% in comparison with a 50% increase in the mean decay time of the FA over the same emission spectral range is measured at $\lambda_{ex}$=314 nm (Table 2).

### 3.2. Time-resolved emission spectra

TRES were reconstructed from 20–21 individual decays as a function of emission wavelength in the range between 390 and 580 nm (bandwidth 9 nm) with a 10 nm spectral step. Fluorescence was excited at 314, 357 and 379 nm and the decays were accumulated up to approx. $3\times10^4$ counts in the peak channel. Each decay curve was fitted with a three-exponential function by using an iterative reconvolution scheme to partially remove the effects of instrumental broadening.

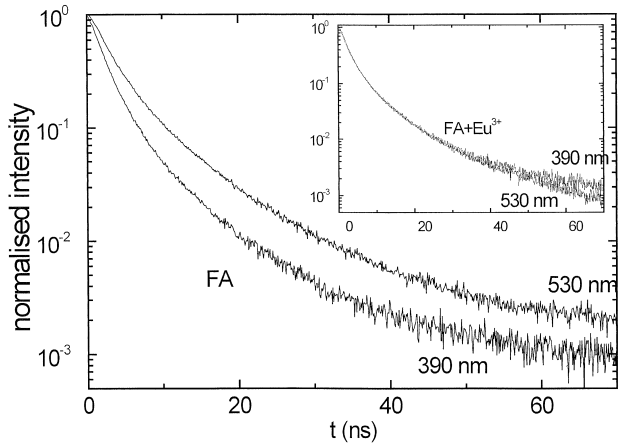


Fig. 4. The fluorescence kinetics of FA excited at 314 nm and measured at 390 and 530 nm emission wavelengths. Insert shows the fluorescence kinetics of FA complexed with $Eu^{3+}$ measured at the same excitation and emission wavelengths. All curves represent the experimental fluorescence decays.

To describe quantitatively the evolution in time of the emission spectra, the experimental spectra were fitted at any time to a log-normal line shape [25]. Two parameters were used: (a) the *barycenter* in frequency, $B(t)$ was computed from the raw spectra and (b) emission maxima $\nu_{max}$ were determined from the log-normal line shape fitted spectra.

In contrast to the single-curve decay analysis, the construction of time-resolved emission spectra has the advantage that the full contour of the emission spectrum obtained from an analytical procedure may lead to a better visualisation of processes occurring in the excited state. This is especially important for the extraction of qualitative and to a less extent quantitative effects on FA fluorescence induced by $Eu^{3+}$ complexation. The analysis of the TRES performed involved at least two steps of non-linear regression which were the fitting of the decay curves at each emission wavelength to a multi-exponential form (to a three-exponential function in our case) and a fitting of the emission spectra at each moment $t$ to a log-normal gaussian line shape function. In more sophisticated approaches of dynamical relaxation, the transient of the spectral shift is also fitted to a multi-exponential form [26]. An error source imposed by our experimental set-up was the normalization of emission spectra [27] because the steady-state emission spectra and TRES were measured on different instruments.

In order to overcome these limitations, all TRES results were discussed only on a comparative basis: TRES were compared either at different excitation wavelengths for the FA, or at the same excitation wavelength for FA and FA complexed with $Eu^{3+}$.

The expression for the log-normal gaussian line shape used in TRES fitting is:

$$I_t(\nu) = \frac{I_0}{1+\beta\Delta\nu}\exp[-\alpha\ln^2(1+\beta\Delta\nu)] \quad (3)$$

with $\Delta\nu=\nu_{max}-\nu$ and $\nu=1/\lambda$ in units of $cm^{-1}$. There are four parameters in the fit: the amplitude at the peak $I_0$, the width and skewness parameters, $\alpha$ and $\beta$, and the frequency at the peak, $\nu_{max}$ (emission maxima). The log-normal distribution is a skewed gaussian distribution (it tends to a gaussian one as ($\beta\Delta\nu\rightarrow0$). Its area, $a$ and full width at half height, $w$ are given by:

$$a = I_0 = [\pi/(\alpha\beta^2)]^{1/2}$$
$$w = [\exp(\delta) - \exp(-\delta)]/[\beta\exp(2\alpha)^{-1}] \quad (4)$$
$$\delta^2 = (2\alpha)^{-2} + (\ln2)/\alpha$$

Due to spectral resolution, no variation in time of the full width at half height, $w$, could be measured at each of the

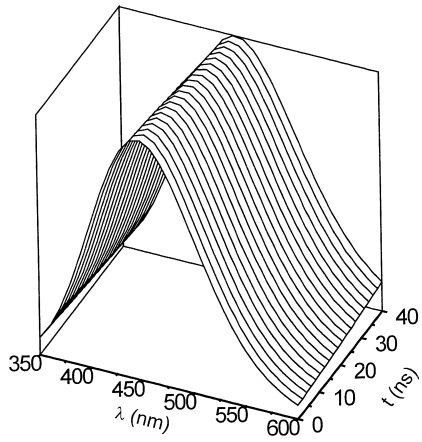


Fig. 5. Three-dimensional representation of a TRES experiment. The smooth curves shown in the graph are the fits of the FA experimental spectra (21 emission wavelengths) to a log-normal line shape function. $\lambda_{ex}$=314 nm and $\Delta t$=2 ns.

three excitation wavelengths. As a consequence, we limited our investigations to one parameter, e.g. the emission maxima, $\nu_{max}$ provided by means of a non-linear least squares routine.

*Time dependence of the barycenter and of the emission maximum of the emission spectra*: The variation of the fluorescence composition with the emission decay rate gave rise to time-evolving spectra shown in Fig. 5.

The curves in Fig. 5 are log-normal fits to the 21-point experimental data at times between 0 and 40 ns, at $\lambda_{ex}$=314 nm, using a temporal step of 2 ns. As can be seen, the fluorescence spectra shifted in time without any noticeable narrowing or changes in shape. A detailed analysis of the spectra, applying a deconvolution with three gaussians, revealed slight variations of line shape and width, nicely illustrated in Fig. 6. No similar behaviour was observed with FA complexed with $Eu^{3+}$, the emission spectra remaining constant in line shape, width and, within spectral resolution, in the position of the maximum intensity (results not shown in the graph).

Thus, the instantaneous emission spectrum was attributed as the envelope of three gaussians with different centres of gravity ($\upsilon_{0i}$) and widths ($\sigma_i$):

$$I(\upsilon,t)=\sum_{i=1}^{3} I_{0i}\exp(-t/\tau_{0i})\times\frac{1}{\sqrt{2\pi}\sigma_i}\times\exp\left(-\frac{[\upsilon_i-\nu_{0i}]^2}{2\sigma_i^2}\right) \quad (5)$$

We must stress that the analysis based on multi-gaussian deconvolution needs to be proven with both a higher spectral and temporal resolution and it is the subject of current work.

*FA*: The evolution in time of the barycenters of the emission spectra at each excitation wavelength is shown in Fig. 7.

Several features of these curves deserve comments: (a) the emission spectra moved in the same sense, e.g., towards

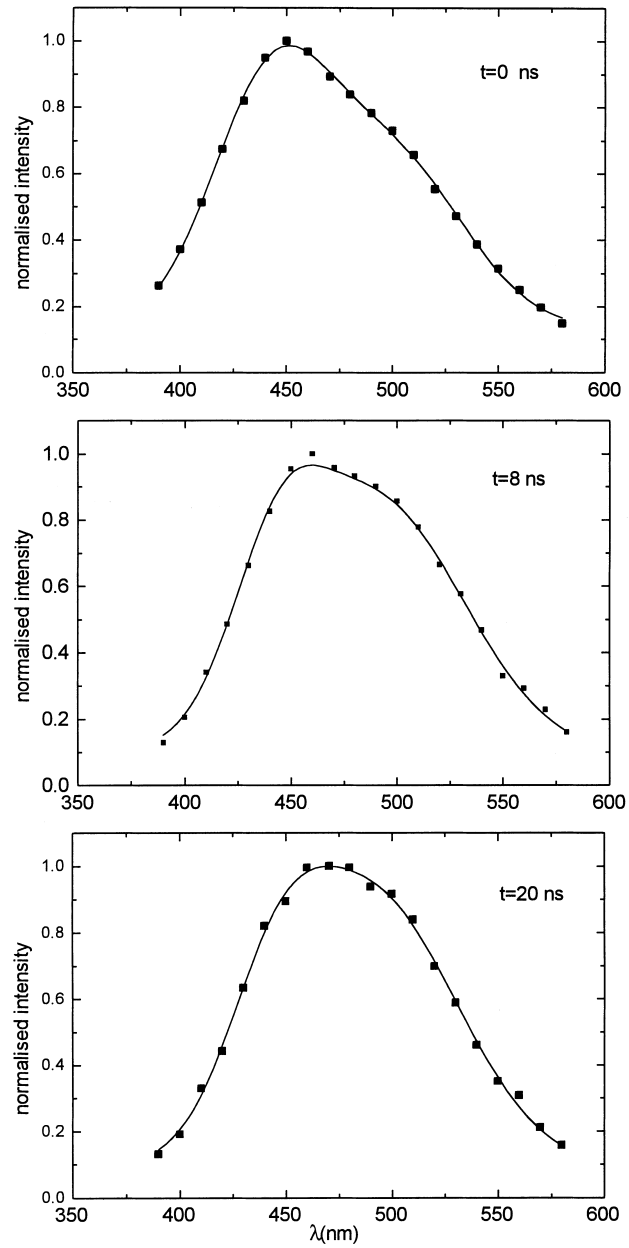


Fig. 6. Time-resolved emisson spectra measured at times of 0, 8 and 20 ns. The smooth curves shown in the graph are the fits of the FA experimental spectra to a three-gaussian line shape function. $\lambda_{ex}$=357 nm.

longer emission wavelengths; (b) the barycenter shifts were quite similar, and they were about 15–20 nm (approx. 600–1000 $cm^{-1}$). Accuracy in determining the emission maxima shifts could be regarded as satisfactory, as these shifts were larger than the spectral resolution (limited to 9 nm); (c) the time dependencies of the barycenters were rather similar for all excitation wavelengths used. There were still some differences: at $\lambda_{ex}$=314 nm, most part of the barycenter shift (more than 60%) was accomplished in the first 3–5 ns, while for the other two excitation wavelengths the same range shifted towards longer times (about 10 ns); (d) The plots of emission maxima and barycenter transients look

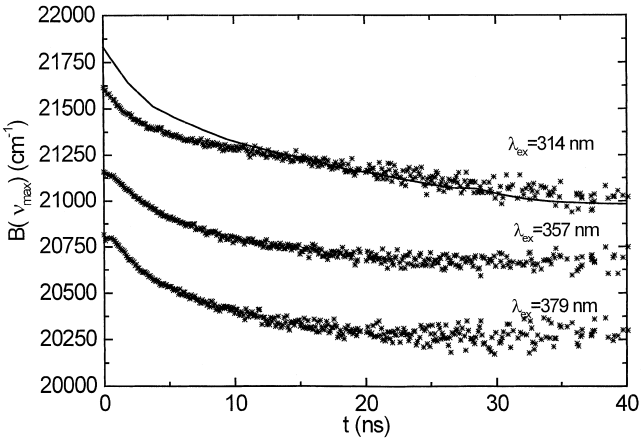


Fig. 7. Evolution with time of the FA emission spectra barycenters at 314, 357 and 379 nm (star curves). For comparison, the evolution with time of the maxima of emission spectra at 314 nm excitation wavelength (see text) is also represented (line curve).

qualitatively similar, suggesting that within our experimental resolution, the spectra did not change noticeably in time in their width and shape, independent of the excitation wavelength. For comparison, in Fig. 7 also the emission maxima transient obtained at $\lambda_{ex}$=314 nm is plotted.

*FA complexed with* $Eu^{3+}$: With the addition of $Eu^{3+}$ the temporal behaviour of the maximum and of the barycenter of emission spectra changed significantly. Within our experimental resolution these changes are consistent with the single decay curve analysis, e.g., showing an almost constant value with time for these two parameters. However, judged on a comparative basis, the trends are clearly different for the TRES of FA and FA complexed with $Eu^{3+}$.

In Fig. 8 the evolution in time of the barycenters of emission spectra of FA and $Eu^{3+}$-bound FA in the first 40 ns after excitation are shown. For comparison purposes only, the $B$ and $\nu_{max}$ measured for FA and $Eu^{3+}$-bound FA at time 0 were normalized.

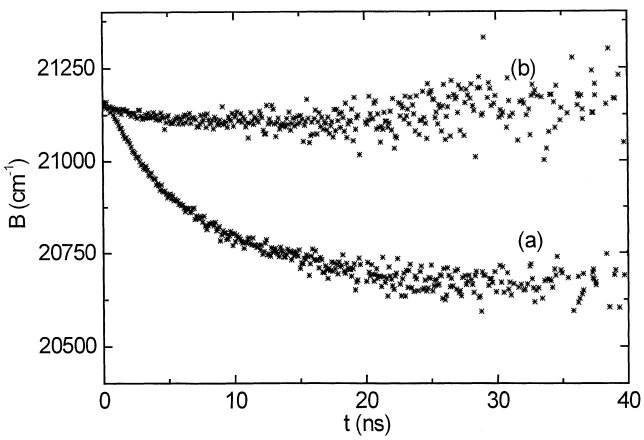


Fig. 8. Evolution with time of the barycenter of emission spectra at 357 nm excitation wavelength: (a) FA complexed with $Eu^{3+}$ and (b) FA.

## 4. Discussion

*FA*: The kinetics behaviour of FA fluorescence showed a strong deviation from mono-exponentiality. Analysis of the multi-exponential decays was performed without restrictions on their number (up to 100 exponential terms were included in ESM analysis) and position. In the great majority of cases, we obtained a three-modal distribution with peak decay time values centred approximately at 0.7, 3 and 10 ns.

The FA fluorescence kinetics was strongly dependent on the emission wavelength, being different at the short and long wavelength sides of emission spectra. These differences were expressed mainly in changes of the relative amplitudes of the decay components while the values of peak decay time may be regarded as constant within experimental and method calculation errors (Table 1). In contrast with emission wavelength dependency, fluorescence kinetics changed only slightly with excitation wavelength (Table 1).

The study of the emission wavelength dependency of the decay curves indicated that a great part of fluorescence decay complexity was due to the inhomogeneous emission decay kinetics determined by ground state heterogeneity effects. Ground state heterogeneity can be expected due to complex mixture of different fluorophores which compose the FA structure on which are superimposed different distributions of environments experienced by each of the fluorophore species. The results indicate that the emission spectrum of FA may be regarded as the superposition of (at least) three broad spectral envelopes, with slightly different emission maxima and widths. It is tempting to attribute the shortest decay time component (approx. 0.7 ns) to the blue edge of the spectral range, where its amplitude was most pronounced. This feature may be regarded as typical for FA of different origins [8].

However, if ground state heterogeneity would be the only factor responsible for the trends in the TRES, one may expect that the amplitude of the short decay time component has a maximum value either at the blue or the red region, depending on the details of the FA structure. Also, fluorescence kinetics would depend more strongly on the excitation wavelength as this dependency is an indication of inhomogenous decay kinetics due to the static effects in the distribution of the excited state species within the initial ensemble of fluorophores. The expected effect would manifest in the enhancement of one of the relative amplitudes of the decay components to the detriment of the other. As shown in Table 1, this is not actually the case, as the value of the relative ratio $A_1/A_2/A_3$ is almost invariant with the excitation wavelength at least in the blue region of the emission range (390–460 nm). As a consequence of the above considerations, one could expect that other processes contribute to the temporal inhomogeneity of FA fluorescence decay as well. These processes may manifest during the excited states decay time of the FA, such as intramolecular and intermolecular rearrangements of the fluorophores

together with a reorganization of fluorophore-solvent hydrogen bonds.

The TRES are very sensitive to both changes of $\tau_i$ and $A_i$ in the course of the relaxation processes [27]. Together with single decay analysis a deeper insight into FA fluorescence decay kinetics was achieved. The time shift of the TRES may be observed even in the case when negative amplitudes are absent (no excited state reactions) or in the absence of the dynamic relaxation process. As discussed in Section 3.1.2, no tendency towards negative values of the relative amplitudes (related to the longest peak decay time) was detected when measuring the kinetics at the red spectral edge. Also, the relaxation process takes place on a time scale much faster than our experimental resolution as the time of the reorientation of the water dipoles is the order of picoseconds, much too fast to be detected with the instrumental set-up used [26].

The TRES data sustain two important conclusions: (a) the fluorescence kinetics of FA depended rather weakly on the excitation wavelength and (b) there were the same fluorophores which contributed to the evolution in time of the emission spectra, whatever excitation wavelength was used. The last conclusion is based on the similar trends with time presented by the barycenters of the emission spectra of FA, at each of the excitation wavelengths (Fig. 7).

Fluorescence spectra shifted in time with slight narrowing and changes in shape (Fig. 6). These aspects of the dynamics may be not intuitive, especially when the ratio of the shortest and longest decay time components has a good contrast value, which is approx. 15 (see Table 1). Thus, one might expect instead that the heterogeneity effects would lead to a narrowing of the spectrum due to the preferential depletion of the short decay time component (situated more or less by coincidence, at the blue spectral edge). That this did not happen in the present case may be due to the fact that we have a superposition (at least) of three broad emission spectra, with closely spaced maxima and similar widths.

*$Eu^{3+}$ complexation effects upon FA fluorescence kinetics*: In the presence of the $Eu^{3+}$, the dependency of the relative amplitudes of the fluorescence decay of the fulvic acid on the emission wavelength was greatly reduced (in comparison with the uncomplexed FA). (Tables 1 and 2 and also the insert in Fig. 4). As expected, for the FA in the presence of $Eu^{3+}$ the mean decay time varied within only 10%, from 7 ns at $\lambda_{em}$=390 nm to 7.7 ns at $\lambda_{em}$=550 nm, whereas in the case of FA the mean decay time varied with almost 50% from 5.2 to 7.5 ns over the same spectral range (Tables 1 and 2).

These results are contrary with what was expected from a dynamic quenching effect, e.g. reduction of the peak decay time values of FA fluorescence in the presence of $Eu^{3+}$. The invariance of the decay time values of the FA fluorescence with $Eu^{3+}$ addition indicates that the effects of $Eu^{3+}$ complexation upon FA fluorescence were not related to energy or/and electron transfer between FA singlet states and the $Eu^{3+}$ ion. Quenching of FA fluorescence induced by $Eu^{3+}$ appeared only static in origin and may have as much to do with its paramagnetic properties as with its spectral properties. Quenching involving the so-called external heavy atom effect reflects efficient singlet–triplet intersystem crossing in FA brought up by an increase in spin-orbit coupling [28]. In our preliminary steady-state experiments the extent of static quenching, $\eta = 1 - I/I_0$ with $I$ and $I_0$ being the fluorescence intensities of $Eu^{3+}$-bound FA and FA, respectively, was around 20% at $\lambda_{ex}$=314 nm.

TRES data confirmed the $Eu^{3+}$ effect upon the relative amplitudes redistribution of FA decay time components. As illustrated in Fig. 8, the barycenter varied almost insignificantly in time, in comparison with the same evolution of FA. This small variation in time of the barycenter may be easily explained if one takes into account the constancy of the peak decay time values and the small variation with the emission wavelength of the corresponding relative amplitudes (Table 2).

In conclusion, single fluorescence decay curve analysis combined with the analysis of the time-resolved emission spectra has been proven to be a powerful method for the investigation of the complex temporal behaviour of FA fluorescence. Results indicated the presence of at least three species of FA fluorophores, each species experiencing its own distribution of chemical environments. The addition of $Eu^{3+}$ induced besides static quenching of the FA fluorescence an invariance of the relative amplitudes of the decay components with the emission wavelength. The peak decay time values of the FA fluorescence in the presence of $Eu^{3+}$ were almost unchanged at all emission and excitation wavelengths investigated. Thus, at this stage it seems to be reasonable to conclude that within the temporal resolution of the experimental set-up used the singlet levels of FA played no role as donor state in intramolecular energy transfer from FA ligands to the upper excited levels of $Eu^{3+}$. Future experiments which will include other quencher ions like $Gd^{3+}$ $Tb^{3+}$ and $Sm^{3+}$ as well as a better correlation between the steady-state and time-resolved emission experiments will attempt to elucidate the specific role of spectroscopic properties of different lanthanide ions in quenching FA fluorescence.

Even though the results have been obtained on the FA fraction of only one NOM sample the spectroscopic approach proved that time-resolved fluorescence experiments can yield valuable information on the molecular dynamics of metal ion complexation by NOM. In future experiments with NOM of different origins and their FA fractions this approach will be further examined.

## Acknowledgements

The authors are grateful to the German Research Foundation (Deutsche Forschungsgemeinschaft, DFG) for their financial support. They appreciate the funding by the German Federal Ministry for Education, Science, Research and Technology (Bundesminesterium fhr Bildung und Forschung, BMBF) as well.

## References


[1] J. Buffle, Complexation Reactions in Aquatic Systems, An Analytical Approach, Ellis Horwood and Wiley, New York, 1988.

[2] R.R. Engebretson, R. Vonwandruska, The effect of molecular size on humic acid associations, Geochem. 26 (1997) 759–767.

[3] J.A. Leenheer, D.M. McKnight, E.M. Thurman, P. McCarthy, Humic substances in the Suwannee river, in: R.C. Averett, D.M. Leenheer, D.M. McKnight, K.A. Throne (Eds.), Georgia: Interaction, Properties and Proposed Structures, Open File Report 87-557, U.S. Geol. Surv., Denver, CO, 1989, p. 331.

[4] Byoung Ho Lee, Kun Ho Chung, Hyun Sang Shin, Yeong Jae Park, Hichung Moon, Europium(III) complexes of polyfunctional carboxylic acids: Luminescence probes of possible binding sites in fulvic acid, J. Colloid and Interface Sci. 188 (1997) 439–443.

[5] J. Buffle, Natural organic matter and metal–organic interactions in aquatic systems, in: H. Siegel (Ed.), Metal Ions in Biological Systems, vol. 18, Marcel Dekker, New York, 1984, pp. 165–221.

[6] M.U. Kumke, H.-G. Löhmannröben, Th. Roch, Fluorescence quenching of polynuclear aromatic compounds by humic acid, Analyst 119 (1994) 997–1001.

[7] Sherry L. Hemmingsen, Linda B. McGown, Phase-resolved fluorescence spectral and lifetime characterization of commercial humic substances, Appl. Spec. 51 (1997) 921–929.

[8] M.U. Kumke, C. Tiseanu, G. Abbt-Braun, F.H. Frimmel, 1998, Fluorescence decay of natural organic matter (NOM)-influence of fractionation, oxidation and metal ion complexation, J. Fluorescence, submitted for publication.

[9] B.J. Colston, J.T. Vanelteren, Z.I. Kolar, J.J.M. Degoeji, Kinetics in a Eu(III)-humic acid system by isotopic exchange with $Eu(152)^{3+}$ and size exclusion chromatography. A feasibility study, Radiochimica Acta 78 (1997) 111–115.

[10] F. Rey, E. Calle, J. Casado, Study of the effects of concentration and pH on the dissociation kinetics of Fe(II)-fulvic acid complexes, Int. J. Chem. Kinetics 30 (1998) 63–67.

[11] J.R. Lead, J. Hamilton-Taylor, M. Kelly, Artifacts in the determination of the binding of americium and europium to aquatic fulvic acid, Sci. Total Environ. 177 (1996) 221–224.

[12] J.I. Kim, R. Klenze, H. Wimmer, W. Runde, W. Hauser, A study of the carbonate complexation of $Cm^{3+}$ and $Eu^{3+}$ by time resolved later fluorescence spectroscopy, J. Alloys and Compounds 213/214, 333–340.

[13] E.K. Legin, Yu.I. Trifonov, M.L. Khokhlov, D.N. Suglobov, Solubilisation of europium fulvate in aqueous solutions containing complexing agents, Radiochemistry 37 (1996) 253–257.

[14] W.Susetyo Thomason, L.A. Carreira, Fluorescence studies of metal–humic complexes with the use of lanthanide ion probe spectroscopy, Appl. Spectr. 50 (1996) 401–408.

[15] M. Nordén, J.H. Ephraim, B. Allard, Europium complexation by an aquatic fulvic acid – effects of competing ions, Talanta 44 (1997) 781–786.

[16] G. Bidoglio, I. Grenthe, P. Qi, P. Robouch, N. Omenetto, Complexation of Eu and Tb ions with Fulvic Acids as Studied by time-resolved laser-induced fluorescence, Talanta 3 (1991) 999–1004.

[17] W.R. Kirk, W.S. Wessels, F.G. Prenergast, Lanthanides-dependent petubations of luminescence in indolylethylenediaminetrtraacetic acid-lanthanide chelate, J. Phys. Chem. 97 (1993) 10326–10340.

[18] S. Speiser, Photophysics and mechanisms of intramolecular electronic energy transfer in bichromophoric molecular systems: Solution and supersonic jet studies, Chem. Rev. 96 (1986) 1953–1976.

[19] T. Foerster, in: O. Sinanoglu (Ed), Modern Quantum Chemistry, Academic, New York, 1964.

[20] W.T. Carnall, The absorption and fluorescence spectra of rare earth ions in solution, in: K.A. Gschneider Jr., L. Eyring (Eds.) Handbook on the Physics and Chemistry of Rare Earths, North-Holland Publishing Company, 1979.

[21] See, for example, I.M. Alaoui, and the references cited herein – Nonparticipation of the ligand's first triplet state in intramolecular energy transfer in $Eu^{3+}$ and $Tb^{3+}$ Ruhemann's Purple complexes. J. Phys. Chem. 99 (1995) 13280–13282.

[22] J.I. Kim, G. Buckau, G.H. Li, H. Duschner, N. Psarros, Characterization of humic and fulvic acids from Gorleben groundwater. Fresenius J. Anal. Chem. 338 (1990) 245–252.

[23] W.R. Ware, Recovery of fluorescence lifetime distributions in heterogenous systems, in: V. Ramamamurthy (Ed.), Photochemistry in Organized and Constrained Media, VCH Publishers, New York, Chem. Phys. Lett. 126 (1991) 7–11.

[24] A. Semiarczuk, B.D. Wagner, W.R. Ware, Comparison of the maximum entropy method and exponential series method for the recovery of distributions of the lifetimes from fluorescence lifetime data, J. Phys. Chem. 94 (1990) 1661–1667.

[25] A. Ord Stuart, K.J. Kendall's, 1987. In Advanced Theory of Statistics, 5th ed., Oxford University Press, New York, vol. 1.

[26] M. Vincent, J. Gallay, A.P. Demchenko, Relaxation around the excited state of indole: Analysis of fluorescence lifetimes distributions and time-dependence spectral shifts, J. Phys. Chem. 99 (1995) 14931–14941.

[27] J.R. Lakowicz, Principles of Fluorescence Spectroscopy, Plenum Press, New York, 1983.

[28] A. Abragam, B. Bleaney, Electron paramagnetic resonance of transition ions, Oxford University, Oxford, 1970.